

EDGE ARTICLE

View Article Online
View Journal | View IssueCite this: *Chem. Sci.*, 2021, 12, 569

All publication charges for this article have been paid for by the Royal Society of Chemistry

Intramolecular Friedel–Crafts alkylation with a silylium-ion-activated cyclopropyl group: formation of tricyclic ring systems from benzyl-substituted vinylcyclopropanes and hydrosilanes†

Tao He,^{ID} Guoqiang Wang,^{ID} Peng-Wei Long,^{ID} Sebastian Kemper,^{ID} Elisabeth Irran,^{ID} Hendrik F. T. Klare^{ID*} and Martin Oestreich^{ID*}

A trityl-cation-initiated annulation of benzyl-substituted vinylcyclopropanes (VCPs) with hydrosilanes is reported. Two Si–C(sp³) bonds and one C(sp²)–C(sp³) bond are formed in this process where an intramolecular 6-*endo-tet* Friedel–Crafts alkylation of a silylium-ion-activated cyclopropane ring is the rate-determining key step. The reaction mechanism is proposed based on computations and is in agreement with experimental observations. The new reaction leads to an unprecedented silicon-containing 6/6/5-fused ring system. A phenethyl-substituted VCP derivative yields another unknown tricycle having 6/6/6 ring fusion by reacting in a related but different way involving a 6-*exo-tet* ring closure.

Received 7th October 2020
Accepted 28th October 2020

DOI: 10.1039/d0sc05553k

rsc.li/chemical-science

Introduction

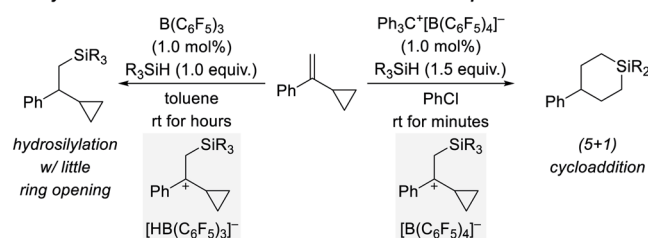
We recently became interested in the reactivity of catalytically generated silicon electrophiles towards cyclopropane derivatives.^{1–3} Our investigations typically comprise B(C₆F₅)₃/hydrosilane combinations⁴ and silylium-ion-like reactants⁵ emerging from hydrosilanes and the trityl salt Ph₃C⁺[B(C₆F₅)₄][–] as an initiator. VCPs as substrates specifically caught our attention because these versatile building blocks can react in diverse ways.⁶ This is also true for their reactions with silicon electrophiles (Scheme 1, top).^{2,3} These reactions involve the intermediacy of β-silicon-stabilized⁷ cyclopropylcarbinylium cations⁸ with different counteranions (gray boxes). Depending on the hydride source, the outcomes could not be more different. For aryl-substituted VCPs, the B(C₆F₅)₃-catalyzed hydrosilylation proceeds generally with little ring opening (top left).² In contrast, treatment of these VCPs with Ph₃C⁺[B(C₆F₅)₄][–] in the presence of various hydrosilanes affords silicon-containing six-membered rings as a result of a formal (5 + 1) cycloaddition accompanied by an aryl migration (top right).³ The situation changes again when replacing the aryl substituent by a benzyl group (Scheme 1, bottom). The hydrosilylation under B(C₆F₅)₃ catalysis is now plagued with ring opening, likely due to poorer stabilization of the carbocation intermediate (bottom left).² Strikingly, the silylium-ion-promoted

setup gives rise to yet another product where the aryl group becomes part of the product's ring system (bottom right). We report here a new trityl-cation-initiated cycloaddition of benzyl-substituted VCPs and hydrosilanes involving an intramolecular Friedel–Crafts alkylation. Our study includes a full experimental and computational mechanistic analysis.

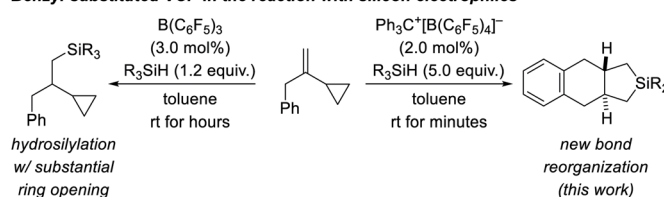
Results and discussion

Using 2 mol% of Ph₃C⁺[B(C₆F₅)₄][–] as an initiator, we began investigating the reaction of VCP **1a** and excess Et₂SiH₂ (**2a**) in

Phenyl-substituted VCP in the reaction with silicon electrophiles



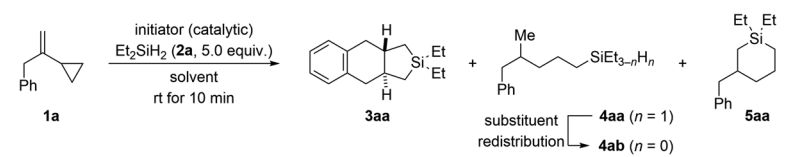
Benzyl-substituted VCP in the reaction with silicon electrophiles



Scheme 1 Diverse outcomes from the reaction of phenyl- and benzyl-substituted VCPs and hydrosilanes (R₃SiH = 3°, 2°, and 1° hydrosilanes with R = alkyl and/or aryl).

Institut für Chemie, Technische Universität Berlin, Strasse des 17. Juni 115, 10623 Berlin, Germany. E-mail: hendrik.klare@tu-berlin.de; martin.oestreich@tu-berlin.de

† Electronic supplementary information (ESI) available: Experimental details, characterization, crystallographic and computational data. CCDC 2034954. For ESI and crystallographic data in CIF or other electronic format see DOI: 10.1039/d0sc05553k

Table 1 Optimization of the trityl-cation-initiated cycloaddition^a


Entry	Initiator (mol%)	Solvent	Yield ^b (%)		
			3aa	4aa/4ab	5aa
1	Ph ₃ C ⁺ [B(C ₆ F ₅) ₄] [−] (2.0 mol%)	Benzene	51	34	9
2 ^c	Ph ₃ C ⁺ [B(C ₆ F ₅) ₄] [−] (2.0 mol%)	Toluene- <i>d</i> ₈	61	26	9
3 ^d	Ph ₃ C ⁺ [B(C ₆ F ₅) ₄] [−] (2.0 mol%)	Benzene	41	47	8
4 ^e	Ph ₃ C ⁺ [B(C ₆ F ₅) ₄] [−] (1.0 mol%)	Benzene	28	28	<5
5	Ph ₃ C ⁺ [B(C ₆ F ₅) ₄] [−] (5.0 mol%)	Benzene	55	30	13
6 ^f	Ph ₃ C ⁺ [B(C ₆ F ₅) ₄] [−] (2.0 mol%)	Benzene	52	33	11
7	Ph ₃ C ⁺ [B(C ₆ F ₅) ₄] [−] (2.0 mol%)	Chlorobenzene	56	20	14
8	Ph ₃ C ⁺ [B(C ₆ F ₅) ₄] [−] (2.0 mol%)	1,2-C ₆ H ₄ Cl ₂	61	19	9
9	Ph ₃ C ⁺ [B(C ₆ F ₅) ₄] [−] (2.0 mol%)	Toluene- <i>d</i> ₈	65	21	13
10	Et ₃ Si ⁺ [CHB ₁₁ H ₅ Br ₆] [−] (2.0 mol%)	Toluene- <i>d</i> ₈	50	23	25
11	[(C ₆ H ₆)·H] ⁺ [CHB ₁₁ H ₅ Br ₆] [−] (2.0 mol%)	Toluene- <i>d</i> ₈	48	26	23

^a All reactions were performed with VCP **1a** (0.10 mmol) and the indicated amounts of the initiator and Et₃SiH₂ (**2a**) under argon atmosphere in the indicated arene solvent (0.5 mL, 0.2 M) at room temperature. Unless otherwise noted, conversion was greater than 95% for each entry as estimated by ¹H NMR spectroscopy using CH₂Br₂ as an internal standard. ^b Yields were estimated by ¹H NMR spectroscopy using CH₂Br₂ as an internal standard and tend to be too high because of the long relaxation time of CH₂Br₂. ^c 1.0 equiv. of norbornene used. ^d 2.0 equiv. of Et₃SiH₂ (**2a**) used. ^e 39% of VCP **1a** recovered. ^f Performed at 0.1 M.

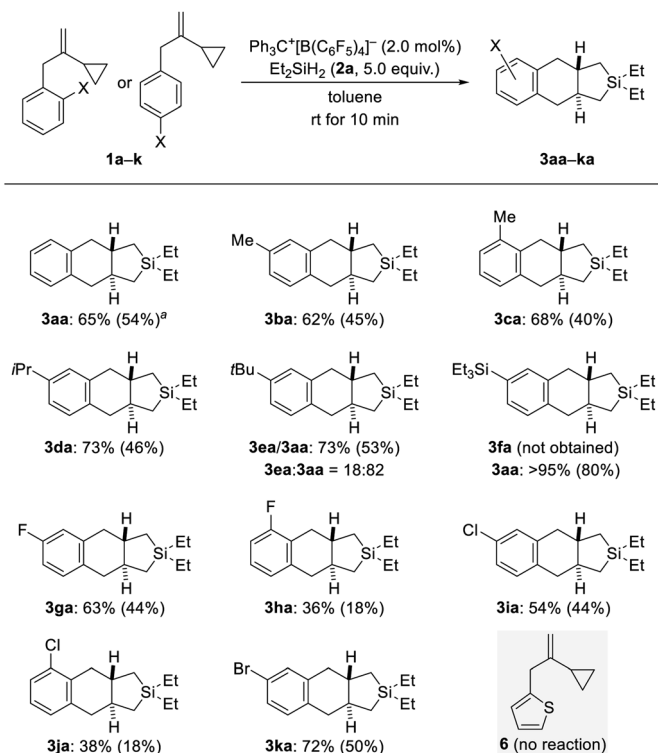
various arene solvents at ambient temperature (Table 1). In benzene as solvent, 2,2-diethyl-2,3,3a,4,9,9a-hexahydro-1*H*-naphtho[2,3-*c*]silole (**3aa**) was found as the major product along with ring-opened 4-methyl-5-phenylpentyl-substituted silane **4ab** and six-membered ring system **5aa** (entry 1). As ring-opening hydrosilylation would yield an unsaturated compound,¹ we speculated that the formation of saturated **4ab** (through initially formed **4aa**)^{9,10} involves an additional alkene hydrogenation by protonation of the VCP to form a cyclopropylcarbiny cation followed by hydride transfer from the hydrosilane. The proton could be released from a Wheland intermediate in the course of an assumed Friedel–Crafts reaction. Addition of norbornene as a proton scavenger had no effect though (entry 2). In turn, the silicon-containing ring system **5aa** could be the result of the aforementioned silylium-ion-promoted hydrosilylation of cyclopropanes¹ coupled with an *endo* cyclization of an allylbenzene intermediate (see discussion of the mechanism).

A diminished yield was observed at a lower loading of the dihydrosilane (2.0 instead of 5.0 equiv.; entry 3). Poor conversion was seen with less initiator; the product distribution was also affected unfavorably at 1.0 mol% catalyst loading (entry 4). More of Ph₃C⁺[B(C₆F₅)₄][−] was without effect (entry 5). Likewise, the reaction outcome did not change at lower concentration (0.1 M instead of 0.2 M; entry 6). The solvent had a minor effect on the ratio of **3aa**, **4ab**, and **5aa** (entries 7–9), and we eventually proceeded with toluene for the highest overall yield. In accordance with our mechanistic picture, both the counteranion-stabilized silylium ion Et₃Si⁺[CHB₁₁H₅Br₆][−] (ref. 11) and the benzenium ion [(C₆H₆)·H]⁺[CHB₁₁H₅Br₆][−] (ref. 12) could also

be used to initiate this cycloaddition, yet with more pronounced formation of undesired cyclic **5aa** (entries 10 and 11).

With the optimized protocol in hand (Table 1, entry 9), we probed the substrate scope (Schemes 2–4). Electronic and steric effects of the substituent on the aryl group were examined with VCPs **1a–k** (*ortho* and *para*, Scheme 2) and **1l–o** (*meta*, Scheme 3). Parent VCP **1a** afforded the cycloadduct **3aa** in 54% isolated yield. Yields were moderate for VCPs with aryl rings bearing an electron-donating methyl or isopropyl group; the position of the substituent made no difference (**1b–d** → **3ba–da**). VCP **1e** decorated with a *tert*-butyl group did participate equally well but underwent predominant de-*tert*-butylation¹³ to mainly afford **3aa** rather than **3ea**. Similarly, Et₃Si-substituted **1f** suffered complete desilylation¹⁴ with none of **3fa** being formed. Interestingly, the isolated yield of 80% for **3aa** was significantly higher than that obtained for the parent system (54% for **1a** → **3aa**). We explain this with loss of a silylium ion instead of a proton, thus eliminating the aforementioned formation of the saturated byproducts **4aa** and **4ab**. This finding not only provides a solution of how to bypass unwanted alkene protonation but is also evidence for the intermediacy of Wheland complexes and as such a Friedel–Crafts-type mechanism. Halogen atoms were tolerated in this reaction but there was a clear difference between *ortho*- and *para*-substituted VCP derivatives (**1g–k** → **3ga–ka**). Yields were moderate for the *para*- and low for the *ortho*-halogenated substrates (the preparation of the *ortho*-bromine-substituted VCP was unsuccessful). Both electronic and steric effects could be responsible for that. Besides, we also subjected VCP **6** with a thien-2-yl instead of the phenyl group to the procedure but did

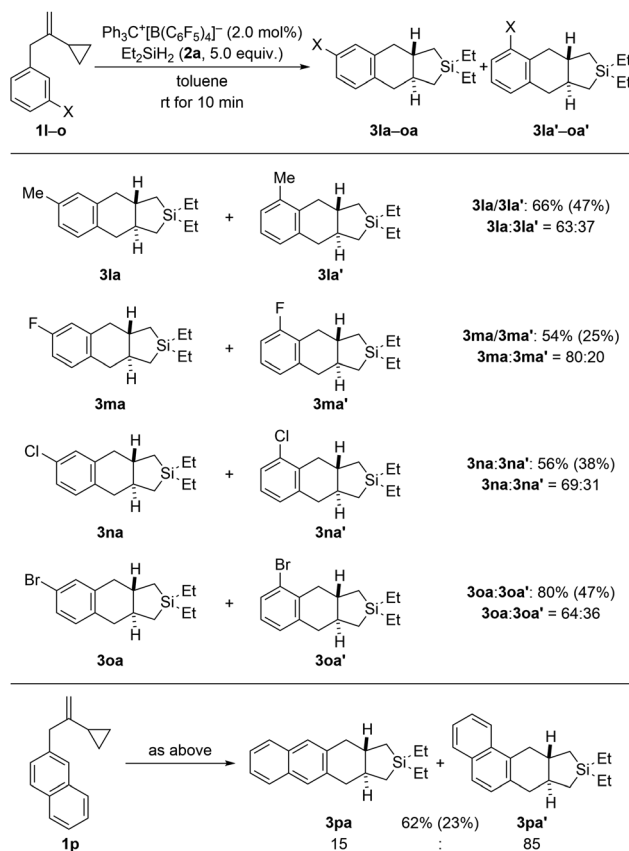




Scheme 2 Scope I: variation of the *ortho*- and *para*-substituent of the benzyl group in VCPs **1**. All reactions were performed on 0.30 mmol scale unless noted otherwise. Conversion was generally greater than 95% as estimated by ^1H NMR spectroscopy using CH_2Br_2 as an internal standard. Yields were estimated by ^1H NMR spectroscopy using CH_2Br_2 as an internal standard and tend to be too high because of the long relaxation time of CH_2Br_2 ; isolated yields in parentheses are of analytically pure material after flash chromatography on silica gel. ^a65% (48%) on a 1.2 mmol scale.

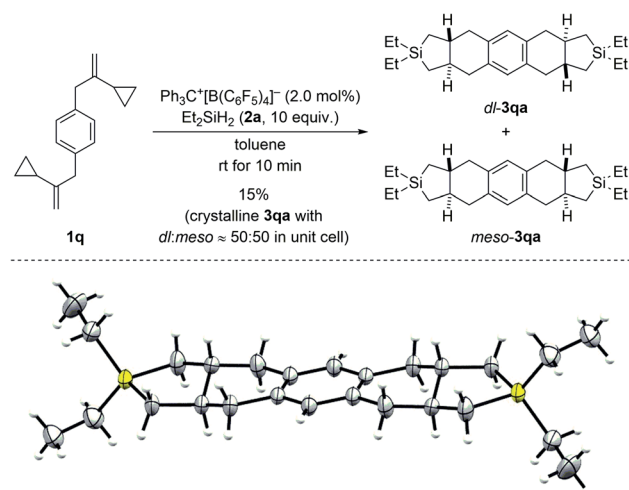
not obtain the cycloadduct; **6** was almost completely recovered (gray box, Scheme 2).

Regioisomeric mixtures of the cycloadducts were generated when starting from representative VCPs with *meta*-substituted aryl groups (**1l-o** \rightarrow **3la-oa/3la'-oa'**, Scheme 3, top). Bond formation occurred preferentially in the less hindered *ortho*-position with regioisomeric ratios ranging from 63 : 37 to 80 : 20. Conversely, VCP **1p** with a naphth-2-yl group yielded the kinetically favored, more hindered cycloadduct **3pa'** with good regiocontrol (Scheme 3, bottom). The cycloaddition of a bis(vinylcyclopropane) system was also tested (**1q** \rightarrow **3qa/3qa'**, Scheme 4, top); *para*-substituted **1q** would first convert into a *meta,para*-disubstituted intermediate (not shown) which, in turn, would then give rise to a mixture of the regioisomers **3qa** and **3qa'** (not shown) in the second cycloaddition event. A complex reaction mixture was experimentally found, and the separation by various chromatography methods failed. Part of the problem is that **3qa** is formed as a mixture of racemic *dl* and *meso* diastereomers in approximately 50 : 50 ratio; the same likely applies to regioisomeric **3qa'** which we were not able to isolate (not shown). Slow evaporation of a solution of that regio- and diastereomeric mixture (four compounds; assuming only *trans* and no *cis* annulation) in ethyl acetate and cyclohexane



Scheme 3 Scope II: variation of the *meta*-substituent of the benzyl group in VCPs **1**. See caption of Scheme 2 for further details. Regioisomeric ratios determined by ^1H NMR spectroscopy after purification.

(1 : 1) eventually led to the co-crystallization of bis-*trans*-isomers *dl*-**3qa** and *meso*-**3qa**. The *meso* compound is depicted in Scheme 4 (bottom; see the ESI† for details).¹⁵ The relative



Scheme 4 Scope III: reaction of a bis(VCP) system (top; see caption of Scheme 2 for further details) and molecular structure of the bis-*trans*-isomer *meso*-**3qa** (bottom; thermal ellipsoids are shown at the 50% probability level).

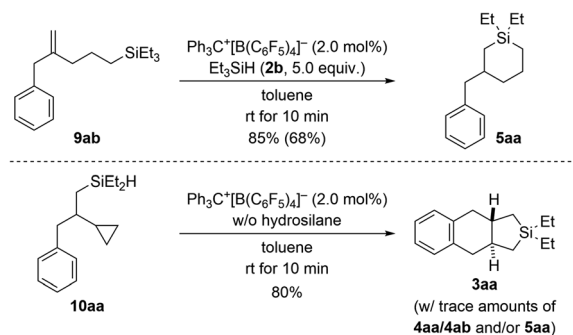


configuration of all annulation products was deduced from this molecular structure and assigned as *trans*, thereby confirming the result obtained from recorded and simulated ^1H NMR spectra.

In our previous study (see Scheme 1, top right),³ we had already shown that, apart from dihydrosilanes, monohydrosilanes can be used with similar success. The reason for this is the ability of silylium ions to cleave $\text{Si}-\text{C}(\text{sp}^3)$ as well as $\text{Si}-\text{C}(\text{sp}^2)$ bonds,^{16,17} corresponding to an exchange of alkyl or aryl group between two silicon centers.⁹ Hence, when there is no $\text{Si}-\text{H}$ bond available (as in a quaternary silane) an alkyl or aryl group can be abstracted by another silylium ion (*cf.* the ESI^+ of ref. 3). We therefore tested a few tertiary hydrosilanes (**2b–d**) in the cycloaddition of model VCP **1a** (Scheme 5). As expected, Et_3SiH (**2b**) afforded the same product **3aa** as obtained with Et_2SiH_2 (**2a**) albeit in lower yield. Demethylation was again preferred over cleavage of an ethyl group with EtMe_2SiH (**2c**). Dearylation occurred when employing Me_2PhSiH (**2d**). These observations are in line with those made earlier.^{3,16,17}

The results with the phenyl-substituted VCPs³ and those with a benzyl substituent (see Scheme 1, bottom) underscore the structural richness that becomes accessible with this chemistry. We had already reported that the corresponding VCP with a cyclohexyl group led to a complex reaction mixture.³ However, going from a benzyl to a phenethyl group was successful, yielding yet another unknown silicon-containing ring system (**7** \rightarrow **8a**, Scheme 6). The relative configuration was deduced from the $^3J_{\text{H,H}}$ coupling (10.6 Hz) in the ^1H NMR spectrum of the highlighted H nuclei.

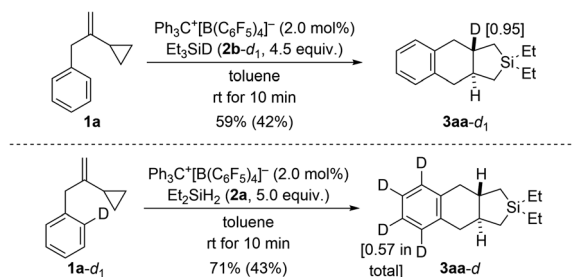
To gain insight into the reaction mechanism, we designed control experiments to distinguish between reaction pathways with the ring opening of the cyclopropyl group happening before or after manipulation of the alkene (Scheme 7). We showed before that silylium-ion-promoted ring-opening



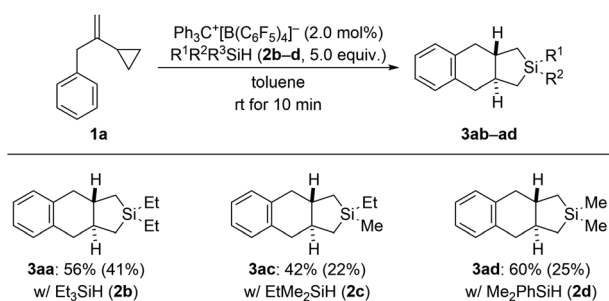
Scheme 7 Control experiments I: verification of ring opening of the cyclopropyl group in VCPs prior to engagement of the alkene unit. See caption of Scheme 2 for further details.

hydrosilylation of cyclopropanes is feasible¹ but had excluded this possibility for phenyl-substituted VCPs³ in the (5 + 1) cycloaddition (see Scheme 1, top right). If hydrosilylation of the cyclopropyl group in VCPs **1** is the initial step, 2-substituted allylbenzene derivatives **9** are likely intermediates. When subjecting independently prepared **9ab** to the standard procedure using Et_3SiH (**2b**), an *endo* cyclization furnished product **5aa** in high yield (top). With **5aa** being formed as minor byproduct in the annulation reaction (*cf.* Table 1), we can state that ring opening preceding the functionalization of the alkene in the VCP is a competing pathway. In turn, potential intermediate **10aa**² arising from alkene hydrosilylation of VCP **1a** and Et_2SiH_2 (**2a**) transformed cleanly into the cycloadduct **3aa** upon treatment with trityl borate $\text{Ph}_3\text{C}^+[\text{B}(\text{C}_6\text{F}_5)_4]^-$ in the absence of external hydrosilane (bottom). Hence, the opening of the cyclopropyl ring is interlinked with the intramolecular Friedel-Crafts-type bond formation at the aryl group¹⁸ and is downstream to the alkene hydrosilylation.

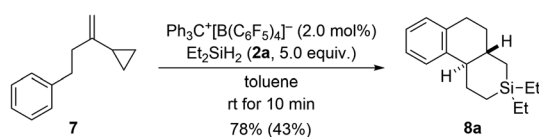
In another set of control experiments, we employed deuterium-labeled hydrosilane Et_3SiD (**2b-d**₁) and model VCP **1a-d**₁ with an *ortho*-C–D bond (Scheme 8). When **1a** was reacted with **2b-d**₁, the deuterium label was exclusively incorporated into one of the angular positions of cycloadduct **3aa-d**₁ (top). To verify whether cleavage of the *ortho*-C–H bond is involved in the rate-determining step, **1a-d**₁ was subjected to the standard setup (bottom). However, H/D scrambling had occurred at all positions of the phenylene group in **3aa-d**.¹⁹



Scheme 8 Control experiments II: deuterium-labeling of the hydrosilane or the VCP. See caption of Scheme 2 for further details. The deuteration grades were estimated by NMR spectroscopy.



Scheme 5 Scope IV: variation of the hydrosilane in the cycloaddition of VCP **1a**. See caption of Scheme 2 for further details.



Scheme 6 Scope V: going from benzyl to phenethyl in the VCP. See caption of Scheme 2 for further details.



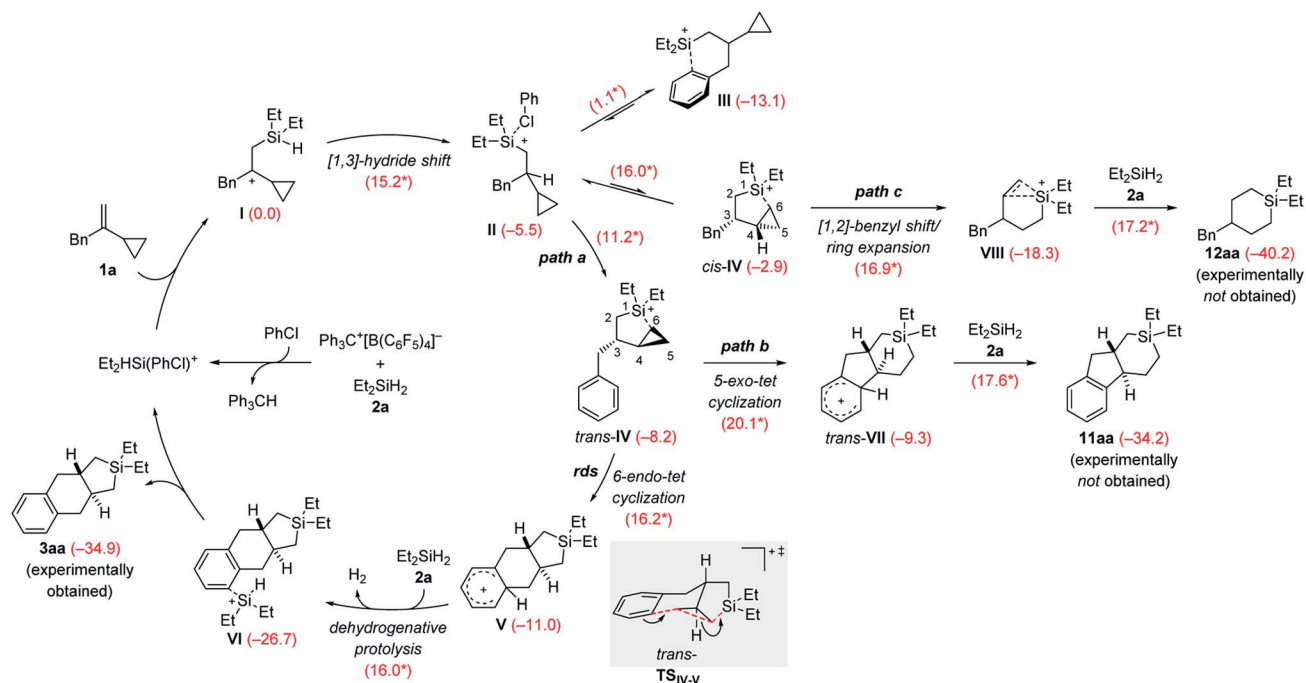
The rough mechanistic picture was refined by density functional theory (DFT) calculations at the M062X/cc-PVTZ//M062X/6-31G(d,p) level.²⁰ Computations were performed on the model reaction of VCP **1a** and Et₂SiH₂ (**2a**) with Ph₃C⁺[B(C₆F₅)₄][−] as the initiator (Scheme 9; see the ESI† for details and Fig. S85 and S86† for the free-energy profiles and the optimized structures). The solvent effect was taken into consideration using a polarizable continuum model (PCM)²¹ for both geometry optimizations and single-point energy calculations. Chlorobenzene was chosen to avoid the complexity of possible proton exchange between Wheland intermediates and toluene. The cycloadduct **3aa** is obtained in moderate yield in chlorobenzene (Table 1, entry 7). We have previously shown that β-silicon-stabilized cyclopropylcarbinyl cation **I**, generated from the association of VCP **1a** and the hydrogen-substituted silylium ion [Et₂HSi(PhCl)]⁺, is much more stable than other donor-stabilized silylium ions such as the corresponding chlorobenzene-, hydrosilane-, or cyclopropane-stabilized systems.³ Unless otherwise noted, adduct **I** is considered the reference minimum for the estimation of the relative energy of intermediates or transition states calculated here.

The β-silylcarbenium ion **I** then undergoes an intramolecular [1,3]-hydride shift from the silicon atom to the benzylic carbon atom to arrive at the chlorobenzene-stabilized silylium ion **II** over a barrier of 15.2 kcal mol^{−1}. We also calculated the potential intermolecular hydride transfer from Et₂SiH₂ (**2a**) to **I** but this pathway can be excluded because of an energetically higher transition state (19.0 *versus* 15.2 kcal mol^{−1}, Fig. S84 in the ESI†). Subsequent reorganization can lead to several intramolecularly donor-stabilized silylium ions **III**

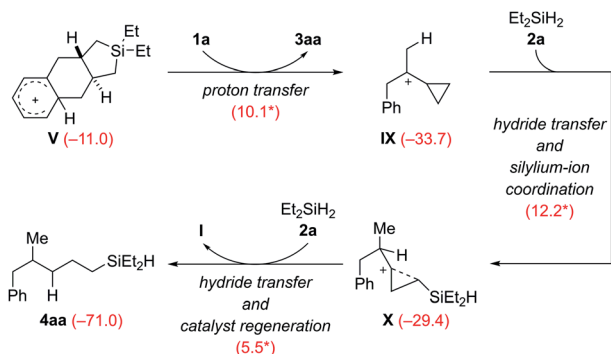
(arene stabilization; see ref. 16*b* for a crystallographically characterized derivative) and *cis*-**IV**/*trans*-**IV** (cyclopropane stabilization with *cis*- or *trans*-configuration). In the case of benzyl-substituted VCPs, **III** is much more stable than either of the two cyclopropane-stabilized silylium ions **IV**. Conversion of **III** into *cis*-**IV** or *trans*-**IV** requires an activation barrier of 16.0 and 11.2 kcal mol^{−1}, respectively. The *trans*-isomer is kinetically and thermodynamically more accessible than the *cis*-isomer. It is therefore *trans*-**IV** which engages in a subsequent intramolecular Friedel-Crafts alkylation reaction of a silylium-ion-activated cyclopropane ring.¹⁸

A 6-*endo-tet* ring closure by nucleophilic attack of the phenyl group at C5 with concomitant cleavage of the distal C5–C6 bond and formation of a bond between C6 and the silicon atom leads to tricyclic Wheland intermediate **V** (path a). This process through transition state *trans*-**TS**_{IV-V} (gray box) is exergonic by −2.8 kcal mol^{−1} with an activation barrier of 16.2 kcal mol^{−1}. It is also the rate-determining step, consistent with the rapid reaction rate at room temperature. The Brønsted acid **V** reacts with hydrosilane **2a** by dehydrogenative protolysis^{17,22} to form the experimentally obtained product **3aa** via **VI** along with dihydrogen and the chlorobenzene-stabilized silylium-ion catalyst (Δ*G*[‡] = 16.0 kcal mol^{−1}). The overall Gibbs free energy change Δ*G* is −34.9 kcal mol^{−1} (calculated from the Gibbs energy difference between **3aa** and **1a/2a**). Based on transition state *trans*-**TS**_{IV-V}, the predicted relative configuration of **3aa** is *trans*, and is supported by ¹H NMR spectroscopy (³*J*_{H,H} = 11.7 Hz) and was eventually confirmed by X-ray diffraction (Scheme 4, bottom).

We considered other kinetically less favorable pathways such as the 5-*exo-tet* cyclization (path b, cleavage of the proximal



Scheme 9 Catalytic cycle of the silylium-ion-promoted cycloaddition of VCP **1a** and Et₂SiH₂ (**2a**). For each reaction step, the Gibbs free reaction energies and barriers (labeled with an asterisk) in kcal mol^{−1} were computed with the M06-2X functional (see the ESI† for details). rds = rate-determining step.



Scheme 10 Computed pathway of the formation of byproduct 4aa, precursor of 4ab (see discussion of Table 1).

C4–C6 bond leading to 11aa) or [1,2]-benzyl shift/ring expansion (path c, leading to 12aa). Neither 11aa nor 12aa were observed experimentally. The route to 12aa corresponds to the previously reported (5 + 1) cycloaddition of phenyl-substituted VCPs³ (see Fig. S87–S90 in the ESI†). However, the annulation of a phenethyl-substituted VCP 7 to afford the 6/6/6-fused ring system 8a can be explained by a related 6-exo-tet cyclization corresponding to path b (see Schemes 6 and S12 in the ESI† for the computed pathway).

The Wheland intermediate **V** is the proton source in this reaction that can also be the starting point of side reactions. Instead of the above dehydrogenative protolysis of the hydrosilane over a barrier of 16.0 kcal mol^{−1} (**V** → **VI**, Scheme 9), this Brønsted acid can also transfer a proton to the C=C double bond of VCP **1a**, releasing the product **3aa** and the cyclopropylcarbinyl cation⁸ **IX** (Scheme 10). The barrier of this protonation step is only 10.1 kcal mol^{−1} and is as such kinetically competitive. Subsequent hydride transfer from Et₂SiH₂ (**2a**) to **IX** gives a γ-silicon-stabilized carbenium ion **X**. This undergoes hydride abstraction from another molecule of **2a** to yield open-chain product **4aa**; the silylium ion released at the same time forms the β-silicon-stabilized cyclopropylcarbinyl cation **I** with VCP **1a**. This ring-opening hydrosilylation of a cyclopropane promoted by a silylium ion is a known reaction and was recently studied by us in detail.¹ With the low barriers involved, the formation of **4aa** and eventually **4ab** after rapid substituent redistribution^{9,10} cannot be avoided.

Conclusion

The present work showcases that reactions of VCPs with different electrophilic silicon reagents do lead to drastically different outcomes (*cf.* Scheme 1). The substituent on the VCP and the choice of the silicon electrophile together with the counteranion of the β-silicon-stabilized cyclopropyl carbocation intermediates decide their fate. With silylium-ion-like reagents, benzyl- and phenethyl-substituted VCPs lead to silicon-containing 6/6/5- and 6/6/6-fused ring systems, respectively, both of which previously unknown motifs. The corresponding phenyl-substituted VCPs engage in a (5 + 1) cycloaddition under otherwise identical reaction conditions.³ The annulation

sequence is initiated by the trityl cation and then maintained by self-regeneration of the silylium-ion reagent.^{5a} Two Si–C(sp³) bonds and one C(sp²)–C(sp³) bond are formed with an intramolecular Friedel–Crafts alkylation of a silylium-ion-activated cyclopropane ring as the key step (6-endo-tet for 6/6/5 system starting from benzyl-substituted VCP and 6-exo-tet for 6/6/6 system starting from phenethyl-substituted VCP). Given the high number of possible reaction pathways, the chemoselectivity and preference for one product with any of the substrates is remarkable.

Conflicts of interest

There are no conflicts to declare.

Acknowledgements

The work was funded by the Deutsche Forschungsgemeinschaft (DFG, German Research Foundation) under Germany's Excellence Strategy (EXC 2008/1-390540038). G. W. and P.-W. L. thank the China Scholarship Council for a postdoctoral fellowship (2019–2020) and a predoctoral fellowship (2019–2023), respectively. All theoretical calculations were performed at the High Performance Computing Center (HPCC) of Nanjing University. M. O. is indebted to the Einstein Foundation Berlin for an endowed professorship.

Notes and references

- 1 A. Roy, V. Bonetti, G. Wang, Q. Wu, H. F. T. Klare and M. Oestreich, *Org. Lett.*, 2020, **22**, 1213–1216.
- 2 P.-W. Long, T. He and M. Oestreich, *Org. Lett.*, 2020, **22**, 7383–7386.
- 3 T. He, G. Wang, V. Bonetti, H. F. T. Klare and M. Oestreich, *Angew. Chem., Int. Ed.*, 2020, **59**, 12186–12191.
- 4 (a) D. Weber and M. R. Gagné, in *Organosilicon Chemistry: Novel Approaches and Reactions*, ed. T. Hiyama and M. Oestreich, Wiley-VCH, Weinheim, 2019, pp. 33–85; (b) M. Oestreich, J. Hermeke and J. Mohr, *Chem. Soc. Rev.*, 2015, **44**, 2202–2220.
- 5 (a) J. C. L. Walker, H. F. T. Klare and M. Oestreich, *Nat. Rev. Chem.*, 2020, **4**, 54–62; (b) P. Shaykhutdinova, S. Keess and M. Oestreich, in *Organosilicon Chemistry: Novel Approaches and Reactions*, ed. T. Hiyama and M. Oestreich, Wiley-VCH, Weinheim, 2019, pp. 131–170; (c) V. Y. Lee and A. Sekiguchi, in *Organosilicon Compounds*, ed. V. Y. Lee, Academic Press, Oxford, 2017, vol. 1, pp. 197–230.
- 6 (a) J. Wang, S. A. Blaszczyk, X. Li and W. Tang, *Chem. Rev.*, DOI: 10.1021/acs.chemrev.0c00160; (b) M. Meazza, H. Guo and R. Rios, *Org. Biomol. Chem.*, 2017, **15**, 2479–2490; (c) V. Ganesh and S. Chandrasekaran, *Synthesis*, 2016, **48**, 4347–4380; (d) L. Jiao and Z.-X. Yu, *J. Org. Chem.*, 2013, **78**, 6842–6848.
- 7 (a) J. B. Lambert, Y. Zhao, R. W. Emblidge, L. A. Salvador, X. Liu, J.-H. So and E. C. Chelius, *Acc. Chem. Res.*, 1999, **32**, 183–190; for a summary of the chemistry of silyl-substituted carbocations, see: (b) H.-U. Siehl and T. Müller,



- in *The Chemistry of Organic Silicon Compounds*, ed. Z. Rappoport and Y. Apeloig, Wiley, Chichester, 1989, part 2, pp. 595–701.
- 8 For a review, see: (a) Z. Goldschmidt and B. Crammer, *Chem. Soc. Rev.*, 1988, **17**, 229–267; for original work, see: (b) G. A. Olah, D. P. Kelly, C. L. Jeuell and R. D. Porter, *J. Am. Chem. Soc.*, 1970, **92**, 2544–2546; (c) G. A. Olah, C. L. Jeuell, D. P. Kelly and R. D. Porter, *J. Am. Chem. Soc.*, 1972, **94**, 146–156; (d) G. A. Olah and P. W. Westerman, *J. Am. Chem. Soc.*, 1973, **95**, 7530–7531; (e) J. F. Wolf, P. G. Harch, R. W. Taft and W. J. Hehre, *J. Am. Chem. Soc.*, 1975, **97**, 2902–2904; (f) H. Mayr and G. A. Olah, *J. Am. Chem. Soc.*, 1977, **99**, 510–513; (g) K. B. Wiberg, D. Shobe and G. L. Nelson, *J. Am. Chem. Soc.*, 1993, **115**, 10645–10652.
- 9 (a) A. Schäfer, M. Reißmann, A. Schäfer, W. Saak, D. Haase and T. Müller, *Angew. Chem., Int. Ed.*, 2011, **50**, 12636–12638; (b) A. Schäfer, M. Reißmann, S. Jung, A. Schäfer, W. Saak, E. Brendler and T. Müller, *Organometallics*, 2013, **32**, 4713–4722; (c) R. Labbow, F. Reiß, A. Schulz and A. Villinger, *Organometallics*, 2014, **33**, 3223–3226; (d) L. Omann, B. Pudasaini, E. Irran, H. F. T. Klare, M.-H. Baik and M. Oestreich, *Chem. Sci.*, 2018, **9**, 5600–5607.
- 10 The formation of **4ab** with an SiEt₃ group rather than expected **4aa** with an SiEt₂H group can be explained by a known substituent redistribution.⁹ This was confirmed by treatment of an independently prepared sample of **4aa** with 2.0 mol% of Ph₃C⁺[B(C₆F₅)₄][−] at room temperature. Within ten minutes, silane **4ab** (*n* = 0, 25%) was found together with monohydrosilane **4aa** (*n* = 1, 54%) and the cognate dihydrosilane (*n* = 2, 21%; not shown). See the ESI† for details.
- 11 Z. Xie, R. Bau, A. Benesi and C. A. Reed, *Organometallics*, 1995, **14**, 3933–3941.
- 12 (a) C. A. Reed, N. L. P. Fackler, K.-C. Kim, D. Stasko, D. R. Evans, P. D. W. Boyd and C. E. F. Rickard, *J. Am. Chem. Soc.*, 1999, **121**, 6314–6315; (b) D. Stasko and C. A. Reed, *J. Am. Chem. Soc.*, 2002, **124**, 1148–1149; (c) C. A. Reed, K.-C. Kim, E. S. Stoyanov, D. Stasko, F. S. Tham, L. J. Mueller and P. D. W. Boyd, *J. Am. Chem. Soc.*, 2003, **125**, 1796–1804.
- 13 S. A. Saleh and H. L. Tashtoush, *Tetrahedron*, 1998, **54**, 14157–14177 and cited references.
- 14 (a) T. H. Chan and I. Fleming, *Synthesis*, 1979, 761–786; (b) C. Eaborn, *Pure Appl. Chem.*, 1969, **19**, 375–388; see also (c) S. Bähr and M. Oestreich, *Angew. Chem., Int. Ed.*, 2017, **56**, 52–59 and cited references.
- 15 CCDC 2034954 (**3qa**) contains the ESI crystallographic data for this paper.†
- 16 (a) Q. Wu, Z.-W. Qu, L. Omann, E. Irran, H. F. T. Klare and M. Oestreich, *Angew. Chem., Int. Ed.*, 2018, **57**, 9176–9179; (b) Q. Wu, A. Roy, E. Irran, Z.-W. Qu, S. Grimme, H. F. T. Klare and M. Oestreich, *Angew. Chem., Int. Ed.*, 2019, **58**, 17307–17311.
- 17 Q. Wu, E. Irran, R. Muller, M. Kaupp, H. F. T. Klare and M. Oestreich, *Science*, 2019, **365**, 168–172.
- 18 To the best of our knowledge, there is one remotely related example of a cyclopropane ring involved in an intramolecular Friedel–Crafts alkylation: V. Lanke, F.-G. Zhang, A. Kaushansky and I. Marek, *Chem. Sci.*, 2019, **10**, 9548–9554.
- 19 F. Cacace, M. E. Crestoni and S. Fornarini, *J. Am. Chem. Soc.*, 1992, **114**, 6776–6784.
- 20 (a) Y. Zhao and D. G. Truhlar, *Theor. Chem. Acc.*, 2008, **120**, 215–241; (b) Y. Zhao and D. G. Truhlar, *Acc. Chem. Res.*, 2008, **41**, 157–167.
- 21 J. Tomasi and M. Persico, *Chem. Rev.*, 1994, **94**, 2027–2094.
- 22 Q.-A. Chen, H. F. T. Klare and M. Oestreich, *J. Am. Chem. Soc.*, 2016, **138**, 7868–7871 and cited references.

